

# Standard edge detection algorithms versus conventional auto-contouring used for a three-dimensional rigid CT-CT matching

M. Mohammadi<sup>1,2,3\*</sup> and Sh. Nabavi<sup>4,5</sup>

<sup>1</sup>Department of Medical Physics, Faculty of Medicine, Hamadan University of Medical Sciences, Hamadan, Iran

<sup>2</sup>School of Chemistry and Physics, The University of Adelaide, South Australia 5000, Australia

<sup>3</sup>Department Of Medical Physics, Royal Adelaide Hospital, South Australia 5000, Australia

<sup>4</sup>Department Of Computer Engineering, Islamic Azad University, Hamadan Branch, Hamadan, Iran

<sup>5</sup>Faculty of Electrical and Computer Engineering, Shahid Beheshti University, Tehran, Iran

**Background:** To reduce uncertainties of patient positioning, the Computerized Tomography (CT) images acquired at the treatment planning time can be compared with those images obtained during radiation dose delivery. This can be followed during dose delivery procedure as Image Guided radiotherapy (IGRT) to verify the prescribed radiation dose delivery to the target as well as to monitor radiation dose constraints for organ at risks located in the vicinity of tumour region. A method was developed to compare registered rigid CT images with those acquired during treatment procedure. **Materials and Methods:** Several CT images were acquired for a typical Rando phantom at head and neck region. Selecting the CT images as reference, they were then manipulated in translational and rotational directions. The differences in translated and rotated images were evaluated by edge detection algorithms and conventional automatic contouring used in most of current treatment planning systems. Setting of standard edge detection algorithms was investigated and the appropriate one was selected. Applying the selected optimized standard edge detection algorithm and conventional auto-contouring on CT image differences, the characteristics of methods were evaluated. **Results:** Results show that 1 pixel difference in translation and 1 degree in rotation can be recognized for inhomogeneous regions. A significant variation was detected at the bony-soft tissue and air-soft tissue conjunction regions. **Conclusion:** The results obtained from the current study are comparable with those reported using Chamfer algorithm. It is concluded that the current method, can be used to control patient positioning in radiotherapy sessions as a part of Image guided radiotherapy protocols. **Iran. J. Radiat. Res., 2012; 10(3-4): 123-130**

**Keywords:** CT-CT matching, Edge detection algorithms, Image registration, Image guided Radiotherapy.

## INTRODUCTION

The application of imaging technology

and image processing plays an essential role in diagnostic and therapeutic progress in medicine. Among current medical efforts, the radiation oncology is widely involved with advanced imaging technologies due to the developed strategies generally termed Image Guided radiation Therapy (IGRT).

Based on the radiation therapy aim, to deliver a prescribed dose to the cancerous tissues while sparing the surrounding normal tissues, the application of different image modalities for patient positioning for accurate treatment and delineation of the region of interest (ROI) is known to be one of the most chief achievements in current radiotherapy. Although, at the moment, the Computed Tomography (CT) scans are playing the clue role to provide reference images for radiotherapy tasks, other modalities including Magnetic Resonance Imaging (MRI), Nuclear Medicine Imaging, Positron Emission Tomography (PET) are also applied for target volume delineation. In addition, to improve the accuracy of treatment, the target volume is recommended to be monitored during treatment procedure, which can be extended up to 40 treatment sessions. One of the achievements recommended so far, is the comparison of the target volume delineated during treatment planning, with those acquired

### Corresponding author:

Dr. Mohammad Mohammadi,  
Department of Medical Physics, Faculty of Medicine,  
Hamadan University of Medical Sciences, Hamadan,  
Iran.

Fax: +98 811 8380208

E-mail: mohammadi@umsha.ac.ir

during treatment sessions using different approaches. Contouring is still known as one of the best options for region of interest delineation (1-4).

Image Guided Radiotherapy (IGRT), which is a relatively old concept, improved in terms of application of technology recently developed, deals with target volume and other Organ At Risks (OARs) positioning during treatment. Whereas radiotherapy treatments are routinely extended into several fractions, so target volumes are potentially able either to move from original geometric positioning. In addition, the volumes of interest (VOIs) can be modified in shape and volume, during treatment due to tumour shrinkage. In such critical situations, IGRT can be applied as a supportive performance to determine the

position of target volume prior to delivery of radiation. If any significant modification of target positioning is observed, so that the target either partially or completely is out of radiation field, or in a different scenario, organ at risk (OAR) has been moved inside the radiation field, the IGRT achievement results can be used to alter the setting and patient positioning. For IGRT achievements, several image modalities can be applied. Brief potential image modalities are shown in table 1.

The comparison of reference images with those taken during treatment are encountered with several difficulties including image registration and deformed images. The comparison of two/three dimensional images used for treatment planning systems and those acquired during

**Table 1.** A brief history of the use of different image modalities for target positioning procedure.

Image type	Acquisition modality	Outcome	References
Planer images	Conventional Radiography	Margin reduction improvement	(12-15)
	Digitally Reconstructed Radiograph	Target re-positioning	(16-18)
	Nuclear Medicine	PET-based Position localization	(2-4, 19)
	Sonography	2-3 mm target shift	(20, 21)
	On Board Imager	daily kV OBI reduces margins to ~ 2.0 mm.	(22-25)
	Electronic Portal Imaging Device	Less than 1 mm field change/ PTV margin ~ 2 mm	(26, 27)
Three-dimensional image	Conventional CT	1 pixel displacement using Chamfer algorithm	(28-30)
	KVCBCT	PTV margin improvement ~ 40%	(25, 31, 32)
	MVCBCT	Margin reduction (pending patient positioning)	(33)
	MRI	< 1 mm displacement detected	(25)
	PET/SPECT	0.92± 0.27 mm registration error	(4, 34, 35)
Four-dimensional image	4D CT	Accurate 4D Targeting Error, (4DTE) analysis standard PTV volume reduction equal to 37%	(1) (36-38)
	4D CBCT	Conventional 4D CBCT artefacts reduction up to 70%. PTV volume correction and normal tissue dose reduction 21%	(39-43)
	4D PET/CT	4D radiation treatment planning (4D RTP)	(1)

treatment, therefore, can be addressed as one of the main challenging issues in IGRT, so-called image registration. This problem plays more important role for three dimensional imaging techniques, because of more dataset involvement. Image registration has been developed as a processing approach to find the point-by-point correspondence between two image series acquired from an identical patient at different times, using different imaging modalities. In order to recognise the differences and correspondences between reference and evaluated images, the image registration processing is an approach to align images to other corresponding images<sup>(5-8)</sup>. The image registration has a range of applications in many areas such as biosecurity, image similarity measurements, medical imaging, remote sensing, etc. For the time being, several algorithms are introduced for rigid and deformable image registrations<sup>(1, 9-11)</sup>. However, most of algorithms are working in the specific criteria. In addition, they are mostly involved with maximizing the measurements of similarities between a transformed and a fixed image<sup>(7, 8)</sup>.

Discarding deformable image registration, the current study is an effort to indicate the sensitivity of optimized standard edge detection algorithms versus conventional auto-contouring, generally used to define the target for treatment planning systems, to figure out that how much image displacement can be detected using different approaches. During the study, the sensitivity of routine standard edge detection algorithms is investigated for transitional and rotational patient/target movement for 3D images. The study evaluates a different achievement instead of conventional auto-contouring to be closer to the intelligent target segmentation with an acceptable accuracy.

## MATERIALS AND METHODS

In order to prepare reference images, several original CT images were prepared

using a typical Rando phantom at head and neck region. Some of CT slices were then selected as reference CT images. The region of interests at reference CT images were displaced in transitional direction (Horizontal and Vertical) from 1 pixel to 5 pixels as well as an axial rotation was performed around the CT image center for 1 degree to 5 degrees. The difference in transition as well as the difference in rotation of the image was evaluated through edge detection algorithms and conventional auto-contouring using an in-house code written in MATLAB (Math Works, Natick, MA, USA). The setting of standard edge detection algorithms, including the threshold and sensitivity, were investigated and the most sensitive one was then selected for the evaluation of image displacement.

Applying the elected standard edge detection algorithm and auto-contouring on a set of CT image differences (difference of manipulated and reference image ones), the sensitivity of each method were evaluated.

## RESULTS

Figure 1 (a, b and c) illustrates an auto-contouring influence on a CT difference map where a 1 pixel shift has been applied at horizontal, vertical and 1° rotation around the central point of image. As figure shows with the increase of auto-contour sensitivity, the noise increases significantly.

Instead of conventional contouring response, standard edge detection algorithms' responses were evaluated for the same shifts. Among available standard edge detection algorithms, it was found that the "Canny" algorithm, which is one the gradient based edge detection algorithms, results are more accurate and acceptable for high gradient region displacements such as air-tissue, and soft bony tissue inhomogeneities. The results for 6 standard edge detection algorithms for 1 pixel shift in transitional, both horizontal and vertical, and rotational misalignments for a head and neck CT image are shown in figure 2.

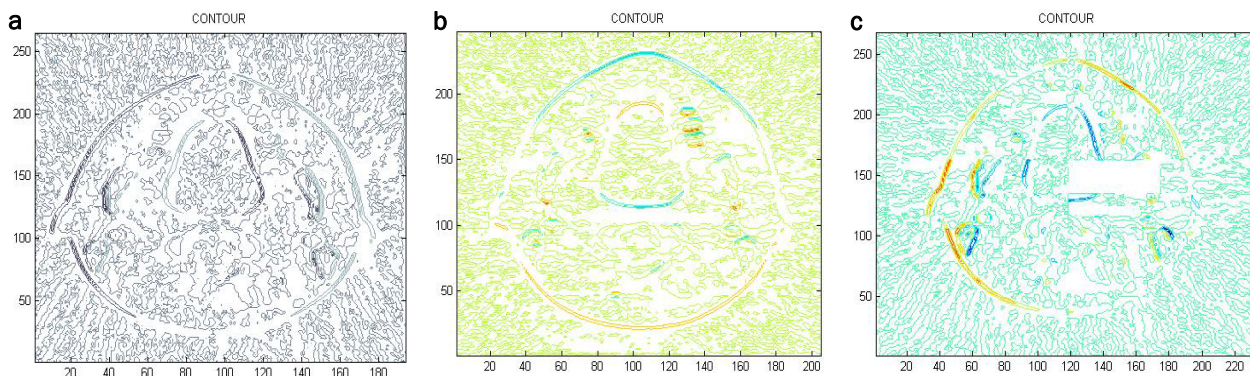


Figure 1. CT image difference after 1 pixel shift in (a) horizontal (b) vertical direction and (c) 1 degree counter clockwise rotation around the CT image centre.

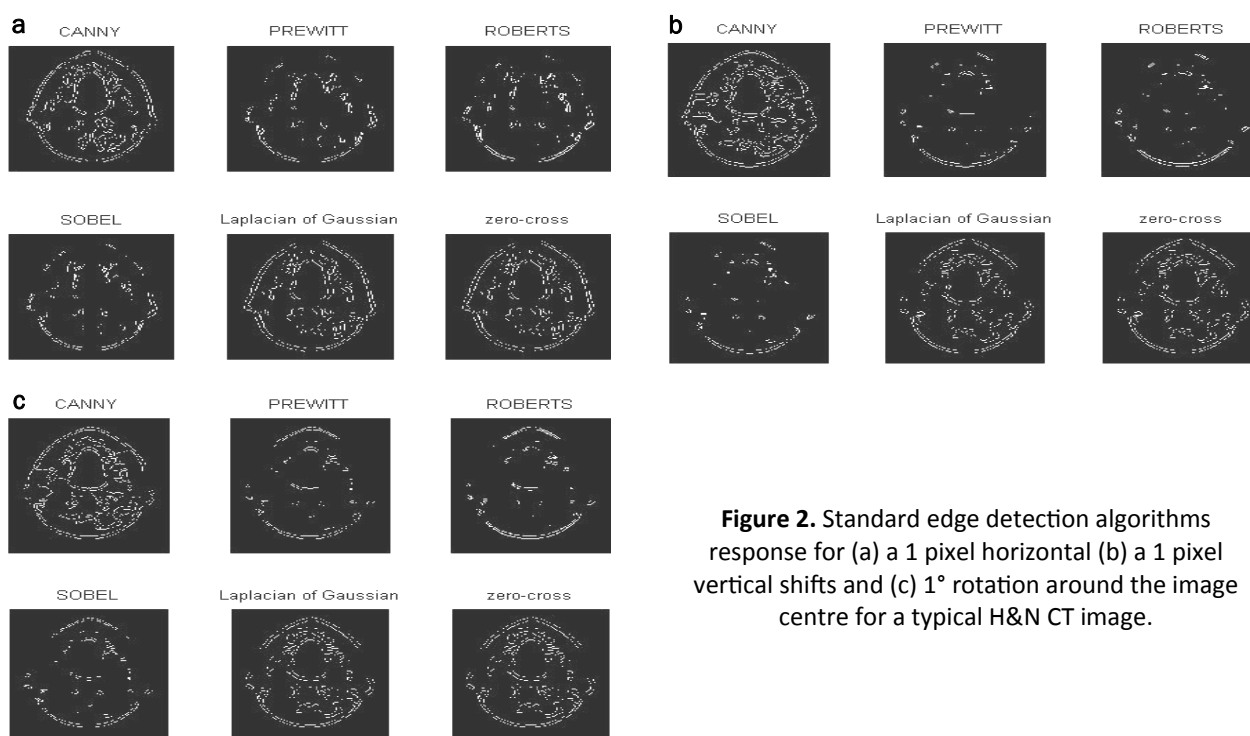


Figure 2. Standard edge detection algorithms response for (a) a 1 pixel horizontal (b) a 1 pixel vertical shifts and (c) 1° rotation around the image centre for a typical H&N CT image.

As results show that the smoothed and optimized auto-contouring used routinely for contouring purposes in treatment planning systems, is not able to detect up to at least 2-3 pixels displacement in high gradient region (figure 3). In contrast, as figure 4 shows, the optimized edge detection algorithm is able to detect the minimum image displacement after image registration. As these figures show, one pixel displacement can be detected using standard edge detection algorithms provided that an appropriate algorithms and setting has been applied.

As final results, the outcome of the current approach can be used to reconstruct a three-dimensional image displacement map which is able to recognize any possible target / organ motion for each slice of images acquired in comparison with reference corresponding images. The technique can be used as a routine check, if new series of CT images are acquired during treatment sessions to compare with the reference ones acquired prior the treatment and used for treatment planning. The three-dimensional image displacement for a 1 pixel horizontal transition and 1 degree image rotation

around the image central point is shown in figure 5. It should also be pointed out that the smallest possible image displacement is 1 pixel, and in this study each pixel size was

0.87 mm. With the increase of image resolution and decreasing each pixel size, more accurate results may be obtained using developed method.

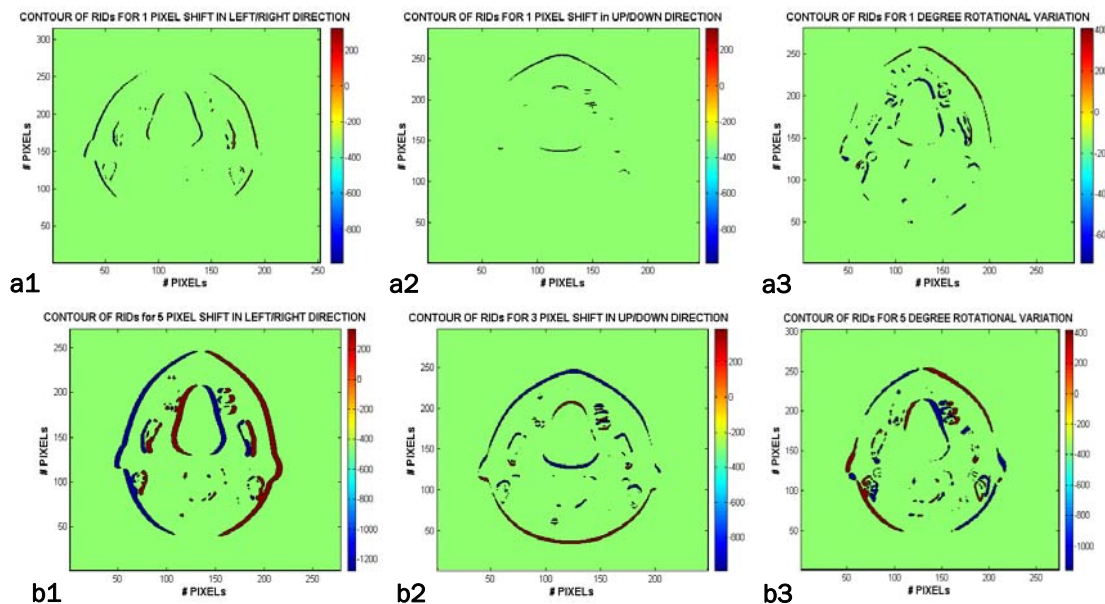


**Figure 3.** Optimized auto-contouring applied to filter undesired contours for uniform areas at a typical CT image difference for 1 pixel shift at (a1) horizontal direction (b1) vertical direction and (c1) 1° rotation around the image central point and for (a2) 5 pixel shift at horizontal direction (b2) 3 pixel shift at vertical direction and (c2) 5° rotation around the image central point.

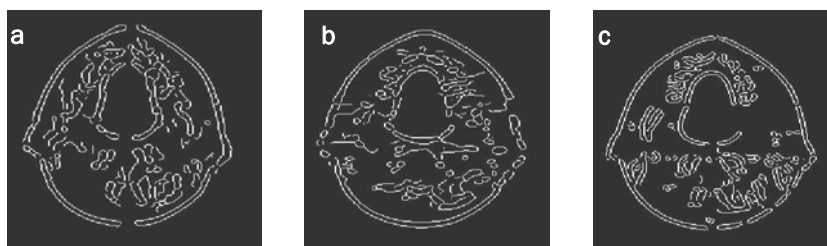


**Figure 4.** The optimized “Canny” edge detection algorithm response applied for CT image difference slices for (a) 1 pixel horizontal and (b) 1 pixel vertical image displacement and (c) 1 degree image rotation around the image centre.

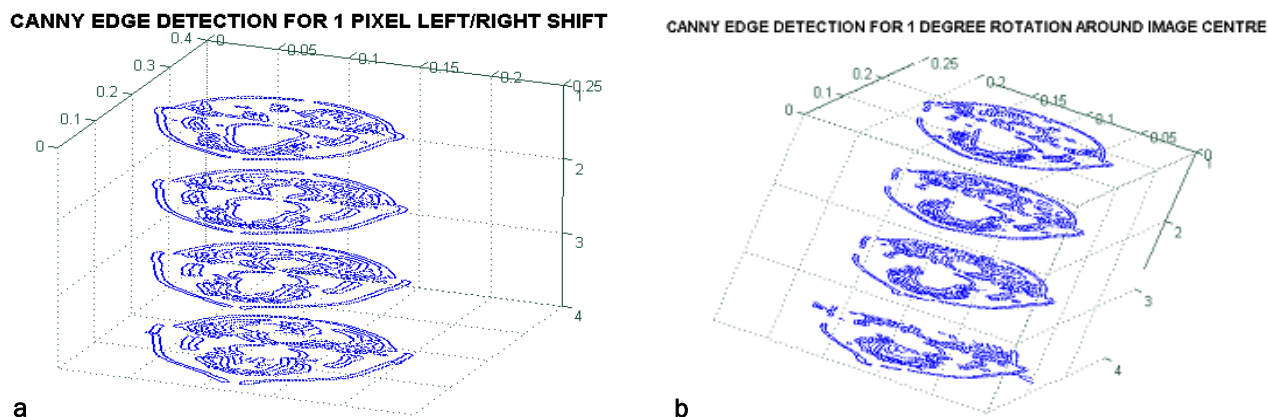


**Figure 5.** Three dimensional reconstructed CT image difference obtained from (a) 1 pixel transitional displacement and (b) 1 degree rotation around the image central point for 4 consecutive CT slices.

## DISCUSSION

As images show in 1 pixel shift (0.87 mm) can be recognized by the conventional auto-contouring method used in most treatment planning systems, provided that the sensitivity of the approach has been increased. However, in some areas the approach is not able to recognise, especially where there is a shift, parallel to the direction of displacement. This decreases the reliability of contouring achievement for small displacements routinely which is the main reason for Image Guided techniques applied for radiation therapy. In addition, as figures show, with the increase of the approach sensitivity, the chance of noise appearance increases significantly. In all three images, the surrounded area for phantom is air and in CT difference map, the reliability of the approach with high sensitivity settings is failed.

As results show, apart from “Canny” algorithm, other gradient based algorithms, such as “Prewitt”, “Roberts”, and “Soble” are not able to recognize small image displacements in the evaluated difference images, even for significant high gradient variations. In contrast, intensity based algorithms such as “Laplacian of Gaussian” and “Zero-cross” approaches showed more reasonable responses compared to gradient based algorithms. However, it should again be noted that the “Canny” assessment was an Exception. Compared to the intensity based algorithms, in the best setting, which will be discussed later, the “Canny” algorithm showed more sensitivity especially in the regions where the displacement were parallel to the shift direction.

All edge detection algorithms require setting for a filter and threshold of action. A “Gaussian” filtration routinely has been applied for first stage. The small filters introduce more blurring and large size filters decrease the sensitivity of the algorithm. In addition, the threshold of action should also be taken into account. According to the

manual of the MATLAB programming software, the manipulation of variable options showed that with the application of a high threshold the important information of displacement will be lost. The investigation also indicated that there is no generic threshold to be used for all images and image modalities<sup>(27, 44, 45)</sup>. This causes an inconvenience of the application of edge detection and up to now there is no automatic or fast approach to find an optimum threshold values. In contrast, with single threshold settings, two thresholds with hysteresis allow more flexibility<sup>(45)</sup>.

The “Canny” algorithm is a filter based on a Gaussian derivation. It is susceptible to noise present on an un-processed image. Compared to other available intensity based algorithms, the “Canny” response is reported to be slightly blurred if an appropriate filter is not applied<sup>(44)</sup>. In addition, as figure 1 show, the high sensitive contouring produces undesired contours in homogenous areas. In order to cope with the problem the sensitivity of the contouring should be optimized. The modified contours for 1 and 5 pixel CT image displacements are shown in figure 5. This shows that after optimizing procedure a 1 mm image displacement can not be detected. Having a reliable outcome from auto-contouring approach, which discards noise level in a uniform area shown in Figure 1, within 3 to 5 pixel image displacement is required to reach a reliable answer, which is shown in figure 3 (b series).

The auto-contouring method generally used in treatment planning systems to delineate target volumes and organ at risks (OARs). In addition, it can be used for patient positioning verification as a part of IGRT package such as Aria (Varian, PALO ALTO, CA, USA), Syngo and Prime-view (Siemens Medical Solution, Germany), and IViewGTTM, XVI software (Elekta Oncology Systems, Stockholm, Sweden). Due to the possible noise in CT images, a routine filtration should be used before any assessment.

However, in some studies, in order to save the image originality especially at high gradient regions, instead of filter or image resizing techniques, other methods may also be applied<sup>(28)</sup>. This study indicates that the automatic contouring with a conventional setting used routinely for image assessment does not present enough accuracy to recognize small image displacement during IGRT procedures and an improvement in contouring algorithms, or the application of other methods should be taken into the considerations.

The results are comparable with routine tools used for rigid image registration<sup>(29, 46-49)</sup>.

## CONCLUSION

The current work concludes that apart from image registration, image comparison using routine auto-contouring can be encountered with several uncertainties. The level of uncertainties sometimes seems to be larger than margins recommended for target and OAR delineations proposed for complicated techniques such as Intensity Modulated Radiotherapy (IMRT). In contrast, edge detection algorithms are shown to be another alternative approach especially in the presence of tissue inhomogeneities. Further investigation is required to evaluate the current algorithm feasibility for soft tissue adjacency, such as prostate cases.

## REFERENCES

- Li G, Citrin D, Camphausen K, Mueller B, Burman C, Mychalczak B, et al. (2008) Advances in 4D medical imaging and 4D radiation therapy. *Technol Cancer Res Treat*, **7**:67-81.
- Lecchi M, Fossati P, Elisei F, Orecchia R, Lucignani G (2008) Current concepts on imaging in radiotherapy. *Eur J Nucl Med Mol Imaging*, **35**: 821-37.
- Song Y, Chan M, Burman C, Cann D (2006) Inter-modality variation in gross tumor volume delineation in 18FDG-PET guided IMRT treatment planning for lung cancer. *Conf Proc IEEE Eng Med Biol Soc*, **1**: 3803-6.
- Heron DE, Smith RP, Andrade RS (2006) Advances in image-guided radiation therapy—the role of PET-CT. *Med Dosim*, **31**: 3-11.
- Sivaramakrishna R (2005) 3D breast image registration—a review. *Technol Cancer Res Treat*; **4**: 39-48.
- Markelj P, Tomazevic D, Likar B, Pernus F. A review of 3D/2D registration methods for image-guided interventions. *Med Image Anal*.
- Makela T, Clarysse P, Sipila O, Pauna N, Pham QC, Katila T, et al. (2002) A review of cardiac image registration methods. *IEEE Trans Med Imaging*, **21**:1011-21.
- Guo Y, Suri J, Sivaramakrishna R (2005) Image registration for breast imaging: a review. *Conf Proc IEEE Eng Med Biol Soc*, **4**: 3379-82.
- Mackie TR, Kapatoes J, Ruchala K, Lu W, Wu C, Olivera G, et al. (2003) Image guidance for precise conformal radiotherapy. *Int J Radiat Oncol Biol Phys*, **56**: 89-105.
- Sarrut D (2006) Deformable registration for image-guided radiation therapy. *Z Med Phys*, **16**: 285-97.
- Wang H, Garden AS, Zhang L, Wei X, Ahamad A, Kuban DA, et al. (2008) Performance evaluation of automatic anatomy segmentation algorithm on repeat or four-dimensional computed tomography images using deformable image registration method. *Int J Radiat Oncol Biol Phys*, **72**:210-9.
- Burnet NG, Adams EJ, Fairfoul J, Tudor GS, Hoole AC, Routsis DS, et al. (2010) Practical aspects of implementation of helical tomotherapy for intensity-modulated and image-guided radiotherapy. *Clin Oncol (R Coll Radiol)*, **22**: 294-312.
- Graf R, Boehmer D, Budach V, Wust P (2010) Residual translational and rotational errors after kV X-ray image-guided correction of prostate location using implanted fiducials. *Strahlenther Onkol*, **186**:544-50.
- Zhang J, Yi B, Lasio G, Suntharalingam M, Yu C (2009) Tomographic image via background subtraction using an X-ray projection image and a priori computed tomography. *Med Phys*, **36**:4433-9.
- Ploquin N, Rangel A, Dunscombe P (2008) Phantom evaluation of a commercially available three modality image guided radiation therapy system. *Med Phys*, **35**: 5303-11.
- Yan H, Ren L, Godfrey DJ, Yin FF. Accelerating reconstruction of reference digital tomosynthesis using graphics hardware. *Med Phys* 2007; **34**:3768-76.
- Lawson JD, Fox T, Elder E, Nowlan A, Davis L, Keller J, et al. (2008) Early clinical experience with kilovoltage image-guided radiation therapy for interfraction motion management. *Med Dosim*, **33**:268-74.
- Carl J, Nielsen J, Holmberg M, Hojkaer Larsen E, Fabrin K, Fisker RV (2008) A new fiducial marker for Image-guided radiotherapy of prostate cancer: clinical experience. *Acta Oncol*, **47**:1358-66.
- White E and Kane G (2007) Radiation medicine practice in the image-guided radiation therapy era: new roles and new opportunities. *Semin Radiat Oncol*, **17**:298-305.
- Leonard CE, Tallhamer M, Johnson T, Hunter K, Howell K, Kercher J, et al. (2010) Clinical experience with image-guided radiotherapy in an accelerated partial breast intensity-modulated radiotherapy protocol. *Int J Radiat Oncol Biol Phys*, **76**: 528-34.
- Huntzinger C, Munro P, Johnson S, Miettinen M, Zankowski C, Ahlstrom G, et al. (2006) Dynamic targeting image-guided radiotherapy. *Med Dosim*, **31**:113-25.
- Godfrey DJ, Yin FF, Oldham M, Yoo S, Willett C (2006)

- Digital tomosynthesis with an on-board kilovoltage imaging device. *Int J Radiat Oncol Biol Phys*, **65**: 8-15.
23. Harmon J, Van Ufflen D, Larue S (2009) Assessment of a radiotherapy patient cranial immobilization device using daily on-board kilovoltage imaging. *Vet Radiol Ultrasound*, **50**: 230-4.
24. Takayama K, Mizowaki T, Kokubo M, Kawada N, Nakayama H, Narita Y, et al. Initial validations for pursuing irradiation using a gimbal tracking system. *Radiother Oncol* 2009; **93**:45-9.
25. Zhu X, Bourland JD, Yuan Y, Zhuang T, O'Daniel J, Thongphiew D, et al. (2009) Tradeoffs of integrating real-time tracking into IGRT for prostate cancer treatment. *Phys Med Biol*, **54**: N393-401.
26. Oyama M, Ueda T, Kitoh S, Goka T, Tanaka T, Ogino T (2006) Evaluation of irradiation position in respiratory-gated radiotherapy using a phantom system simulating patient respiration. *Nippon Hoshasen Gijutsu Gakkai Zasshi*; **62**:1666-74.
27. Mohammadi M and Bezak E (2007) Evaluation of MLC leaf positioning using a scanning liquid ionization chamber EPID. *Phys Med Biol*; **52**:N21-33.
28. Kwa SL, Theuvs JC, van Herk M, Damen EM, Boersma LJ, Baas P, et al. (1998) Automatic three-dimensional matching of CT-SPECT and CT-CT to localize lung damage after radiotherapy. *J Nucl Med*, **39**:1074-80.
29. van Herk M, Gilhuijs KG, de Munck J, Touw A (1997) Effect of image artifacts, organ motion, and poor segmentation on the reliability and accuracy of three-dimensional chamfer matching. *Comput Aided Surg*, **2**:346-55.
30. van Herk M and Kooy HM (1994) Automatic three-dimensional correlation of CT-CT, CT-MRI, and CT-SPECT using chamfer matching. *Med Phys*, **21**:1163-78.
31. Gong Y, Wang J, Bai S, Jiang X, Xu F (2008) Conventionally-fractionated image-guided intensity modulated radiotherapy (IG-IMRT): a safe and effective treatment for cancer spinal metastasis. *Radiat Oncol*, **3**:11.
32. Walter C, Boda-Heggemann J, Wertz H, Loeb I, Rahn A, Lohr F, et al. (2007) Phantom and in-vivo measurements of dose exposure by image-guided radiotherapy (IGRT): MV portal images vs. kV portal images vs. cone-beam CT. *Radiother Oncol*, **85**:418-23.
33. Siddiqui F, Shi C, Papanikolaou N, Fuss M. Image-guidance protocol comparison: supine and prone set-up accuracy for pelvic radiation therapy. *Acta Oncol* 2008; **47**: 1344-50.
34. de Crevoisier R, Isambert A, Lisbona A, Bodez V, Marguet M, Lafay F, et al. (2007) [Image-guided radiotherapy]. *Cancer Radiother*, **11**: 296-304.
35. Yamaguchi S, Ishikawa M, Bengua G, Sutherland K, Nishio T, Tanabe S, et al. (2011) A feasibility study of a molecular-based patient setup verification method using a parallel-plane PET system. *Phys Med Biol*, **56**: 965-977.
36. Riboldi M, Sharp GC, Baroni G, Chen GT (2009) Four-dimensional targeting error analysis in image-guided radiotherapy. *Phys Med Biol*, **54**:5995-6008.
37. Sangalli G, Passoni P, Cattaneo GM, Broggi S, Bettinardi V, Reni M, et al. (2011) Planning design of locally advanced pancreatic carcinoma using 4DCT and IMRT/IGRT technologies. *Acta Oncol*, **50**:72-80.
38. Tanaka R, Mori S, Endo M, Sanada S (2008) Volumetric tracking tool using four-dimensional CT for image-guided-radiation therapy. *Radiol Phys Technol*, **1**: 38-43.
39. Leng S, Zambelli J, Tolakanahalli R, Nett B, Munro P, Star-Lack J, et al. (2008) Streaking artifacts reduction in four-dimensional cone-beam computed tomography. *Med Phys*, **35**:4649-59.
40. Leng S, Tang J, Zambelli J, Nett B, Tolakanahalli R, Chen GH (2008) High temporal resolution and streak-free four-dimensional cone-beam computed tomography. *Phys Med Biol*, **53**: 5653-73.
41. Harsolia A, Hugo GD, Kestin LL, Grills IS, Yan D. Dosimetric advantages of four-dimensional adaptive image-guided radiotherapy for lung tumors using online cone-beam computed tomography. *Int J Radiat Oncol Biol Phys* 2008; **70**:582-9.
42. Cho B, Suh Y, Dieterich S, Keall PJ (2008) A monoscopic method for real-time tumour tracking using combined occasional X-ray imaging and continuous respiratory monitoring. *Phys Med Biol*, **53**: 2837-55.
43. Li T, Koong A, Xing L (2007) Enhanced 4D cone-beam CT with inter-phase motion model. *Med Phys*, **34**: 3688-95.
44. Canny J (1986) A computational approach to edge detection. *IEEE Trans. Pattern Anal. Mach. Intell*, **8**:679-698.
45. Davis L. A survey of edge detection techniques. *CGIP* 1975; **4**:248-270.
46. Cai J, Chu JC, Saxena VA, Lanzl LH (1998) A simple algorithm for planar image registration in radiation therapy. *Med Phys*, **25**: 824-9.
47. Sarkar A, Santiago RJ, Smith R, Kassaei A (2005) Comparison of manual vs. automated multimodality (CT-MRI) image registration for brain tumors. *Med Dosim*, **30**: 20-4.
48. Sykes JR, Brettell DS, Magee DR, Thwaites DI (2009) Investigation of uncertainties in image registration of cone beam CT to CT on an image-guided radiotherapy system. *Phys Med Biol*, **54**:7263-83.
49. van Herk M, Bruce A, Kroes AP, Shouman T, Touw A, Lebesque JV (1995) Quantification of organ motion during conformal radiotherapy of the prostate by three dimensional image registration. *Int J Radiat Oncol Biol Phys*, **33**: 1311-20.